

Investigation of *Acanthus montanus* Leaves Extract as Corrosion Inhibitor for Copper in 2 M Sulphuric Acid

Iniofon Godwin Udom , Grace A. Cookey and Paul Ocheje Ameh

Received: 19 December 2024/Accepted 06 February 2025/Published: 14 February 2025

<https://dx.doi.org/10.4314/cps.v12i3.9>

Abstract: *This study investigates the corrosion inhibition potential of Acanthus montanus leaves extract (AMLE) on copper in 2 M H₂SO₄ solution. Corrosion is a significant issue for materials in industrial environments, leading to material degradation and economic losses. This study aims to explore the use of AMLE as a green inhibitor to mitigate copper corrosion, aligning with the increasing demand for environmentally friendly solutions. The inhibitory performance was evaluated using weight loss measurements, electrochemical polarization, and electrochemical impedance spectroscopy (EIS). Additionally, adsorption and activation studies were conducted to elucidate the inhibition mechanism. In the experimental setup, copper coupons were immersed in 2 M H₂SO₄ containing different concentrations of AMLE (0.1–0.5 g/L). The results reveal that AMLE significantly reduces the corrosion rate of copper, with inhibition efficiency (%IE) increasing with extract concentration. The weight loss method showed a maximum inhibition efficiency of 81.51% at 0.5 g/L of AMLE. However, inhibition efficiency decreased with increasing temperature, suggesting a temperature-sensitive adsorption process. Electrochemical polarization studies indicated that AMLE acts as a mixed-type inhibitor, reducing both anodic and cathodic corrosion reactions. EIS results demonstrated that AMLE functions by forming a protective layer on the copper surface, with charge transfer resistance increasing proportionally with extract concentration. The FT-IR and SEM analyses confirmed the formation of a protective film comprising extract molecules adsorbed onto the copper surface. Activation energy (E_a) values for the inhibited systems were consistently higher than*

those of the uninhibited system, indicating that AMLE reduces the corrosion rate by increasing the energy barrier for the corrosion process. The observed increase in activation energy with extract concentration supports a physical adsorption mechanism. Adsorption studies showed that the process is spontaneous and endothermic, with the data fitting well into the Langmuir isotherm model, further supporting physical adsorption. This study highlights the potential of AMLE as a cost-effective and eco-friendly corrosion inhibitor for copper in acidic environments. The extract's ability to form a stable protective layer and its mixed-type inhibition behavior make it a promising alternative to synthetic inhibitors, particularly in industrial applications where environmental safety is a priority.

Keywords: *Copper, corrosion inhibition, sulphuric acid Acanthus montanus.*

Iniofon Godwin Udom*

Physical Chemistry Unit, Department of Chemistry, Rivers State University, Port Harcourt, Rivers State, Nigeria

Email: iniofonudom123@yahoo.com

Orcid id: <https://orcid.org/0009-0003-6639-3839>

Grace A. Cookey

Physical Chemistry Unit, Department of Chemistry, Rivers State University, Port Harcourt, Rivers State, Nigeria

Email: cookey.grace@ust.edu.ng

Paul Ocheje. Ameh

Physical Chemistry Unit, Department of Chemistry, Nigeria Police Academy Wudil, Kano, Nigeria.

Email: amehpaul99@gmail.com

Orcid id: <https://orcid.org/0000-0002-7050-6715>

1.0 Introduction

Corrosion refers to the deterioration of materials such as polymers (Osabuohien, 2017), metals (Eddy *et al.* 2010), concrete (Sathe & Devsalle, 2025) and other materials. However, corrosion of metal has received a wider and significant research commitment compared to other materials because metals corrodes at a rate faster than other materials. Copper is one of the extensively utilized metals in industries owing to its excellent electrical, thermal and mechanical properties. The metal has good resistance to corrosion and other forms of degradation that supports its functional applications in central heating systems, condensers, oil refineries, transformers and transmission of electricity (Mounir *et al.*, 2012). However, in spite of its numerous advantages and wider scope of applications, several studies have confirmed that in an aggressive environment, copper is still subject to corrosion (Ech-chihbi, *et al.*, 2023). In some industries, such aggressive environments that overcome the resistance of copper to corrosion have been reported during acid wash/cleaning, pickling, descaling and other metallurgical practices (Hart and James 2014)]. Therefore, if the usefulness of copper-based materials must be sustained to enhance industrial and economic productivity, mitigation measures towards the retardation of the corrosion of copper must be fixed and enhanced. [Udom *et al.*, 2018]. Consequently, some reported practical options have been widely recorded in the literature including oiling/greasing, anodic/cathodic protection (Folorunso, 2023). The use of corrosion inhibitors is one of the most valuable method, towards the mitigation of corrosion damages (Eddy *et al.*, 2010; Odoemelam *et al.*, 2009). Corrosion inhibitors are chemical substances that protect metals against corrosion and they often function by adsorbing themselves on the surface of the metals by forming a protective layer (Ebenso *et al.*, 2008; Okoye *et al.*, 2024).

On the highlights of some classes of common corrosion inhibitors are some drugs and pharmaceutical products (Eddy and Ebenso, 2010; Oubahou *et al.*, 2024), Also, some synthetic compounds including Schiff bases (Emrayed *et al.*, 2025), inorganic nanoparticles due to their high surface area (Udongwo, & Folorunso, 2025; Yadav *et al.*, 2024) etc. However, most recent studies have sustained the uniqueness advantages of organic or plant based materials over inorganic corrosion inhibitors because they are less toxic, easily accessible, and could be easily enhanced for higher performance (Bilgic, 2023; Eddy *et al.*, 2024). A large number of plant extracts have been reported as effective corrosion inhibitors for copper in different media. For example, the inhibitive action of *Emblica Officinalis* (AMLA) leaves extract on the corrosion of copper and its alloy in natural sea water has been reported by (Deepa and Selvaraj, 2010) and were found to show good experimental desirability. Also, study conducted by]. . Results observed by Gasari *et al.* (2024) concerning the inhibitive capacity of *Persea americana* extract against copper corrosion indicated an inhibition efficiency of 97%. The success was attributed to the adsorption of the phytochemicals on the metal surface, in consistent with the Langmuir type of adsorption. A mixed type inhibitor characters were also attributed to the inhibitor. It has been reported that *Citrullus colocynthis* fruit extract showed better inhibition efficiency on copper in H₂SO₄, NaOH, and NaCl media [Mohsin *et al.*, 2014]. The inhibitive action of *xanthosoma* Spp leaf extracts (XLE) on copper in seawater [Hart *et al.*, 2016]. [Hart and James, 2014] investigated the inhibitive effect of *Aloe vera Barbadosensis* gel on copper in HCl medium. The extracts *Trigonella stellate* [Fouda *et al.*, 2016], *Capparis spinosa* (CS) leaves [Fadel *et al.*, 2017], *Euphorbia heterophylla* [Fouda *et al.*, 2017] in HNO₃ solutions and *Myrianthus arboeris* leaves in H₂SO₄ solution [Udom *et al.*, 2018] have been



reported to inhibit the corrosion of copper. The inhibition potential of plant extract is generally attributed to the presence of complex organic species, such as; alkaloids, flavonoids, tannins, nitrogen bases, carbohydrates and proteins. A general observation from the listed methods is that the organic compounds functions effectively based on factors such as, the presence of heteroatom, polar functional groups, conjugated bonds, aromatic system and high molecular mass. Arising from the numerous observations recorded as success concerning the employment of plant extracts as corrosion inhibitors, especially concerning the roles of different phytochemicals that could differ in types and concentration for different plant extracts, the need for the continuous investigation of different plant extracts as corrosion inhibitors for metals, including copper is highly desirable. Our previous investigation has shown that *Acanthus montanus* leaves extract was a good inhibitor for the corrosion of aluminium in 2M HCl solution [Udom *et al.*, 2017]. This study focuses on the potency of *Acanthus montanus* leaves extract as corrosion inhibitor of copper in 2M H₂SO₄ solution using weight loss and electrochemical, Fourier transform infrared (FT-IR) and scanning electron microscope (SEM) techniques.

2.0 Materials and Methods

2.1 Preparation of *Acanthus montanus* Leaves Extracts

The fresh leaves of *Acanthus montanus* plant were obtained from Oruk-anam LGA, Akwa Ibom State, Nigeria. The leaves were washed thoroughly and rinsed with deionized water to remove soil impurities, sun-dried and milled to powder. 50g of the finely powdered leaves were placed in a 500 ml round bottom flask containing 99.8% methanol in a soxhlet extractor. The resulting extract was evaporated in an oven at 40°C until drying and then weighed and stored in a sample container for use. The extract was then used for phytochemical analysis. From *Acanthus*

montanus leaves extract the different concentrations of 0.1, 0.2, 0.3, 0.4 and 0.5g/l stock solution were prepared in 2M H₂SO₄ solution and used throughout the present investigation. The aggressive medium was 2M H₂SO₄ prepared from 98% analytical grade supplied by Sigma-Aldrich. All reagents used for this present study were Analar grade and double distilled water was used for the preparation.

2.2 Material Preparation

The copper sheets used for this study were of 0.1cm thickness and 99.5% purity. The copper sheets used for weight loss measurement were mechanically press cut to a rectangular dimension of 5.0 x 2.5cm coupons with a perforated hole at the centre of each coupon to allow hanging with a polymeric thread. For electrochemical methods, the coupons were press cut into 2 x 1.5cm dimensions. The coupons were polished with different sizes of emery paper starting with the coarse to the finest (1200) grade, degreased in absolute ethanol, rinsed with double distilled water and dried with acetone. The treated coupons were then stored in moisture-free desiccators before being used for corrosion studies to prevent contamination.

2.3 Weight Loss Measurements

Weight loss measurements were performed using 250 ml beakers containing 100 ml test solution under total immersion conditions at 303-353K maintained in a thermostat water bath. The pre-cleaned and weighed copper coupons were suspended in beakers using a polymeric thread (Odoemelam *et al.*, 2008).. The coupons were retrieved from the test solution at 2 hrs intervals progressively for 18 hrs, washed with deionized water, rinsed in acetone, dried in air and reweighed. The weight loss in grams was taken as the difference in the weight of the copper coupons before and after immersion in different test solutions. Tests were performed for the blank solution (2M H₂SO₄), *Acanthus montanus* leaves extract concentrations of 0.1–0.5g/l at temperatures of



303-353K. The experiments were done in triplicate to ensure reproducibility. The procedure for weight loss determination was similar to that reported by (Johnathan *et al.*, 2015) as expressed in equation 1 (Eddy & Ita, 2011)

$$\Delta W_{(g)} = W_i - W_f \quad (1)$$

where, ΔW is the weight loss of the copper coupons, W_i is weight before immersion, while W_f is the weight after immersion in the test solution. From the weight loss results, the corrosion rate (CR) and the percentage inhibition efficiency (%IE) values were calculated using the Equations below. The corrosion rates ($\text{gcm}^{-2}\text{h}^{-1}$) of copper in different media were computed using the expression in equation 2 (Eddy & Ebenso, 2008)

$$CR = \frac{\Delta W}{At} \quad (2)$$

where, ΔW_B = weight loss (g), A is surface area (cm^2) of adsorbent and t is the time of immersion (hours). The inhibition efficiency (% IE) was computed using equation 3.

$$\%IE = \left(\frac{\Delta W_B - \Delta W_{inh}}{\Delta W_B} \right) \times 100 \quad (3)$$

where, ΔW_B , ΔW_{inh} are the weight losses of copper in the absence and presence of *Acanthus montanus* leaves extract in H_2SO_4 solution at a particular temperature. The surface of the metal covered by the inhibitor (θ) was evaluated using equation 4.

$$\theta = \left(1 - \frac{W_{inh}}{W_B} \right) \quad (4)$$

2.4 Electrochemical measurements

The electrochemical experiments were performed using a conventional three-electrode Pyrex glass cell with platinum as the counter electrode (CE), the reference electrode was a saturated calomel electrode (SCE), which was coupled to a Luggin capillary. Copper coupons with 0.5cm^2 exposed areas were used as working electrodes (WE). The test electrolytes were 2M H_2SO_4 solution and two different concentrations (0.1 and 0.5 g/l) of the extract.

The experiments were performed using a VERSASTAT 4 Princeton Applied electrochemical analyzer. All electrochemical measurements were carried out at 303K using 100 ml of test solution in a stationary condition. Before each potentiodynamic polarization (PDP) and electrochemical impedance spectroscopy (EIS) measurement, the working electrode was immersed in the test solution for 30 mins until a steady state open circuit potential (Eocp) was established. After measuring the open circuit potential, potentiodynamic polarization curves were obtained with a scan rate of 1mVs^{-1} in the potential range from -0.25 to $+0.25$ mV relative to the Eocp. Corrosion current densities (I_{corr}) values were obtained by extrapolation of anodic and cathodic (β_c and β_a) Tafel lines to corrosion potential. The corrosion inhibition efficiency was evaluated from I_{corr} values by using the relationship;

$$\eta(\%) = \frac{I_{corr}^o - I_{corr}^{inh}}{I_{corr}^o} \times 100 \quad (5)$$

where, I_{corr}^o and I_{corr}^i are the uninhibited and inhibited corrosion current densities respectively.

The electrochemical impedance spectroscopy (EIS) measurements were performed in a frequency range from 100kHz to 10mHz using an amplitude of 5mV peak to peak with ac signals at open circuit potential. The value of R_{ct} was calculated from the Nyquist plot and the inhibition efficiency ($\eta\%$) was computed from the charge transfer resistance R_{ct} values using the relationship;

$$\eta(\%) = \frac{R_{ct}^{inh} - R_{ct}^o}{R_{ct}^{inh}} \times 100 \quad (6)$$

where, R_{ct}^o and R_{ct}^{inh} are the uninhibited and inhibited charge transfer resistance respectively. The double-layer capacitance (C_{dl}) values were calculated using the equation below;

$$C_{dl} = \frac{1}{2\pi f_{max} R_{ct}} \quad (7)$$



where, f_{\max} is the frequency at which the imaginary component of the Nyquist plot is maximum. Each experiment was performed in triplicate to ensure reproducibility.

2.5 Surface Analysis

2.5.1 FR-IT study

Before the experiment, a FTIR study was carried out on the pure sample of AMLE to identify the active functional group. Copper coupons were further immersed in the test solution containing 0.5g/l concentration of the extract for 18 hours. After the corrosion study, the corrosion products were collected with a sample bottle mixed with KBr and then subjected to Fourier transform infrared spectroscopy using SHIMADZU Model IR-8400s Japan spectrophotometer to identify the functional group in the corrosion products.

2.5.2 Scanning Electron Microscopy (SEM) study

Copper coupons were examined before and after exposure to 2M H_2SO_4 solutions for 18 hours in the absence and presence of the extract. Scanning electron microscope (SEM) model JSM-5600 LV was used for this investigation.

3.0 Results and Discussion

3.1 Weight Loss study

The variation in the weight loss of copper coupons immersed in 2M H_2SO_4 solution over

time, with and without various concentrations of AMLE at 303K, is shown in Fig. 1. Similar trends were observed at elevated temperatures (313K–353K). Weight loss was significantly reduced in the presence of AMLE compared to the blank, indicating its corrosion-inhibiting properties. The weight loss decreased as the AMLE concentration increased, highlighting the concentration-dependent nature of its inhibition. For example, at 303K, the corrosion rate (CR) decreased from $7.48 \times 10^{-4} \text{ g cm}^{-2} \text{ h}^{-1}$ in the blank to $1.39 \times 10^{-4} \text{ g cm}^{-2} \text{ h}^{-1}$ at 0.5 g/L AMLE, corresponding to an inhibition efficiency (%IE) of 81.51%.

The data in **Table 1** further illustrate this concentration-dependent effect across all studied temperatures. For instance, at 313K, the corrosion rate dropped from $10.05 \times 10^{-4} \text{ g cm}^{-2} \text{ h}^{-1}$ in the blank to $2.13 \times 10^{-4} \text{ g cm}^{-2} \text{ h}^{-1}$ at 0.5 g/L AMLE, with an inhibition efficiency of 78.81%. Similarly, at 353K, the corrosion rate in the blank was $16.72 \times 10^{-4} \text{ g cm}^{-2} \text{ h}^{-1}$, while the same concentration of AMLE reduced it to $6.73 \times 10^{-4} \text{ g cm}^{-2} \text{ h}^{-1}$, corresponding to an inhibition efficiency of 59.76%. These results confirm that higher AMLE concentrations enhance surface protection by increasing the degree of surface coverage (θ), which ranged from 0.70 to 0.81 at 303K and 0.46 to 0.59 at 353K for extract concentrations of 0.1–0.5 g/L.

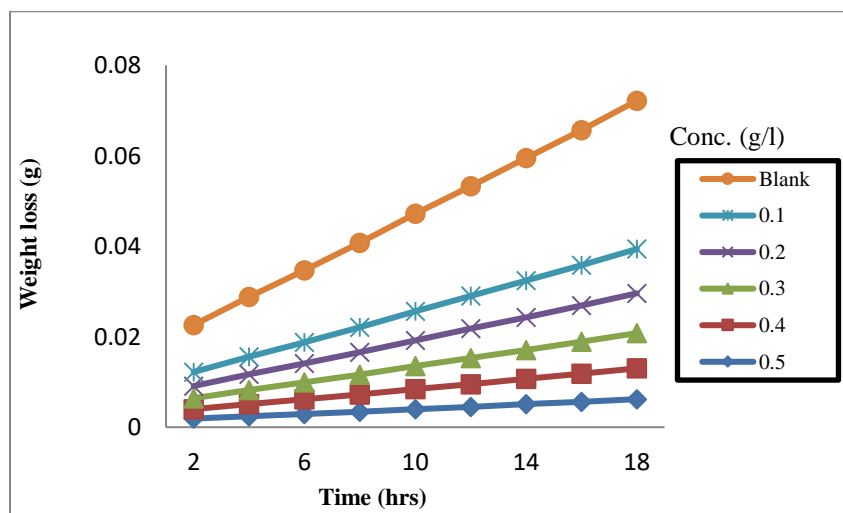


Fig. 1: Variation of weight loss (g) with time (hrs) for Copper coupons in 2M H_2SO_4



with various concentrations of the extract at 303K.

The influence of temperature on the inhibition efficiency is depicted in Fig. 2. The data reveal an inverse relationship between inhibition efficiency and temperature, indicating that higher temperatures reduce the protective effect of AMLE. For instance, at a concentration of 0.5 g/L, the inhibition efficiency dropped from 81.51% at 303K to 59.76% at 353K. This decrease suggests that the interaction between AMLE molecules and the copper surface is predominantly physical, as higher temperatures likely disrupt the adsorbed protective layer.

The progressive increase in inhibition efficiency with extract concentration demonstrates that more AMLE molecules adsorb onto the copper surface at higher concentrations, forming a more extensive

protective layer and reducing corrosion rates. Conversely, the decline in inhibition efficiency with temperature indicates desorption or breakdown of the adsorbed molecules as thermal agitation increases. These observations are consistent with earlier studies by Udom et al. (2017) and Abiola et al. (2016), which attributed such behavior to the thermal instability of physically adsorbed plant extract molecules.

Finally, AMLE acts as an effective corrosion inhibitor for copper in 2M H₂SO₄ its efficiency is concentration-dependent but inversely related to temperature. These findings highlight the potential of AMLE as an eco-friendly corrosion inhibitor, with maximum efficiency achieved at lower temperatures and higher extract concentrations.

Table 1: Corrosion Rate (CR), Inhibition Efficiency (%IE), and Surface Coverage (θ) of Various Inhibitor Concentrations at Different Temperatures

Parameter	Blank	0.1 g/L	0.2 g/L	0.3 g/L	0.4 g/L	0.5 g/L
CR (303K) ($\times 10^{-4}$ g cm ⁻² h ⁻¹)	7.48	2.22	1.99	1.77	1.54	1.39
CR (313K) ($\times 10^{-4}$ g cm ⁻² h ⁻¹)	10.05	3.26	2.98	2.68	2.36	2.13
CR (323K) ($\times 10^{-4}$ g cm ⁻² h ⁻¹)	11.45	4.41	4.07	3.74	3.51	3.26
CR (333K) ($\times 10^{-4}$ g cm ⁻² h ⁻¹)	14.39	6.55	6.13	5.71	5.26	4.82
CR (353K) ($\times 10^{-4}$ g cm ⁻² h ⁻¹)	16.72	9.08	8.41	7.73	7.22	6.73
%IE (303K)	—	70.32	73.40	76.44	79.46	81.51
%IE (313K)	—	67.52	70.43	73.36	76.63	78.81
%IE (323K)	—	61.46	64.47	67.38	69.42	71.60
%IE (333K)	—	54.51	57.41	60.39	63.51	66.54
%IE (353K)	—	45.73	49.69	53.74	56.81	59.76
θ (303K)	—	0.70	0.73	0.76	0.79	0.81
θ (313K)	—	0.67	0.70	0.73	0.77	0.79
θ (323K)	—	0.61	0.64	0.67	0.69	0.71
θ (333K)	—	0.54	0.57	0.60	0.63	0.66
θ (353K)	—	0.46	0.49	0.54	0.57	0.59

As seen in Table 1, there is a progressive increase in inhibition efficiency as the concentration of the extract increased. This indicates that more AMLE components are adsorbed on the copper surface at higher concentrations, leading to greater surface coverage. The inhibition efficiency decreased

with an increase in the temperature of the reaction medium, suggesting that the interaction of the extracted molecule with the copper surface is physical. Similar observations have been reported by [Udom *et al.*, 2017; Abiola *et al.*, 2016] to be due to the breakdown of the adsorbed components of the



extract molecules on the copper surface as the temperature rises.

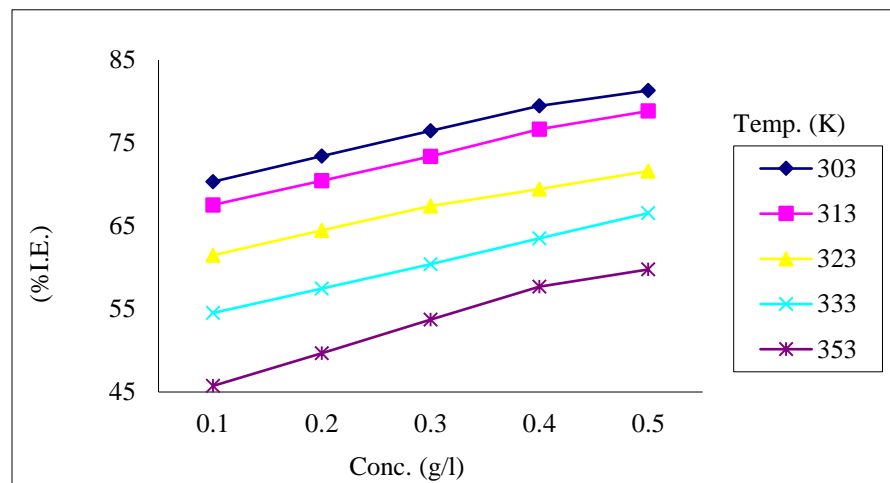


Fig. 2: Variation of percentage inhibition efficiency (%IE) with AMLE concentration (g/l) for the corrosion of copper coupons in 2M H₂SO₄ at different temperatures

3.2 Adsorption Considerations

The adsorption characteristics of AMLE were investigated by fitting the experimental data obtained for the degree of surface coverage (θ) into different adsorption isotherms, including Freundlich, Temkin, and Langmuir models. Linear regression coefficients (R^2) were used to determine the best fit. It was observed that the experimental data adhered most strongly to the Langmuir adsorption isotherm across all temperature ranges studied.

The Langmuir isotherm is described by Equation (8):

$$\frac{C}{\theta} = \left(\frac{1}{K_{ad}}\right) + C \tag{8}$$

where, C is the inhibitor concentration, θ is the degree of surface coverage and K_{ads} is the adsorption equilibrium constant. Straight-line plots of $\frac{C}{\theta}$ versus CCC (Fig. 3) were obtained, with the Langmuir isotherm showing the highest R^2 value of 0.999, indicating a strong adherence to the model. From the intercepts of the straight lines, the values of K_{ads} were computed.

The computed values of K_{ads} and the corresponding free energy of adsorption ($-\Delta G_{ads}$) are presented in Table 2.

Table 2. Langmuir Parameters for the Adsorption of AMLE on Copper Surface

Temp. (K)	K_{ad}	$-\Delta G$ (kJ/mol)	R^2
303	1.49	11.13	0.99
313	1.44	11.41	0.99
323	1.43	11.75	0.99
333	1.49	12.23	0.99
353	1.44	12.87	0.99

The relationship between the standard free energy of adsorption (ΔG_{ads}) and the equilibrium constant (K_{ads}) is give in equation (9):

$$\Delta G_{ad} = -2.303RT \log(55.5K) \tag{9}$$

As shown in Table 2, the values of K_{ads} decreased with an increase in temperature, indicating that the adsorption of AMLE on the copper surface is more favorable at lower temperatures. The negative values of ΔG_{ads} confirm the spontaneous nature of the adsorption process and suggest a physical adsorption mechanism. According to literature,



negative ΔG_{ads} values around -20 kJ/mol or lower are consistent with electrostatic interactions between charged molecules and a charged metal surface (physical adsorption),

while values around -40 kJ/mol or higher suggest chemical adsorption involving charge sharing or transfer to form a coordinate bond

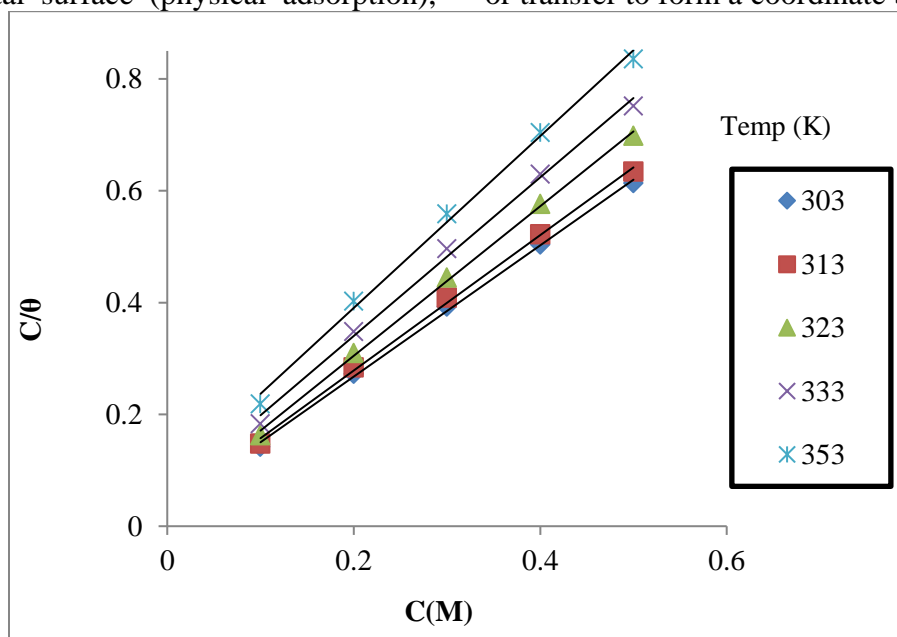


Fig. 3. Langmuir adsorption plot of (C/θ vs C) for inhibition of copper in 2 M H₂SO₄ by different concentrations of AMLE at temperatures of 303-353K

3.3 Thermodynamic investigation

The apparent activation energy values (E_a) for the corrosion process in the absence and presence of AMLE were calculated from the Arrhenius equation as expressed in equation 10

$$\log CR = \log A - \left(\frac{E_a}{2.303RT} \right) \quad (10)$$

where, CR is the corrosion rate, E_a is the apparent activation energy, T is the absolute temperature, R is the universal gas constant and A is the Arrhenius pre-exponential factor.

Fig. 4 shows the Arrhenius plot ($\log CR$ vs $\frac{1}{T}$) for copper in 2M H₂SO₄ solution in the absence and presence of different concentrations of the AMLE. Straight lines were obtained with a slope of $-E_a/2.303R$. The values of E_a were calculated from the slope of the Arrhenius plot and are presented in Table 3. The result shows that the E_a value in the absence of the extract is 12.12 kJ/mol and the highest value of

27.56 kJ/mol⁻¹ in the presence of 0.5g/l of the extract. Higher E_a values for inhibited solutions suggest that the adsorbed extract molecules have formed a thin coat on the copper surface that has become a barrier for mass/charge transfer from the surface to the electrolyte [Ijuo *et al.*, 2016; Namrata *et al.*, 2015]. It has been reported Alaneme and Olusegun 2012; Ameh and Eddy, 2018)icates chemical adsorption, while, E_a less than 80 kJ/mol⁻¹ shows physical adsorption. Hence, the adsorption of AMLE molecules on the copper surface occurred according to the physical adsorption mechanism.

The enthalpy ΔH^* and entropy ΔS^* of activation for the corrosion reaction of copper in 2M H₂SO₄ solution in the absence and presence of different concentrations of AML extract were calculated using the transition state theory equation expressed in equation (11) [Udom *et al.*, 2017; Abeng *et al.*, 2017].

$$\log \frac{CR}{T} = \left(\log \frac{R}{Nh} + \frac{\Delta S}{2.303RT} \right) - \frac{\Delta H}{2.303RT} \quad (11)$$



where, CR is the corrosion rate at temperature T, R is the molar gas constant, N is Avogadro's constant, and h is Planck's constant.

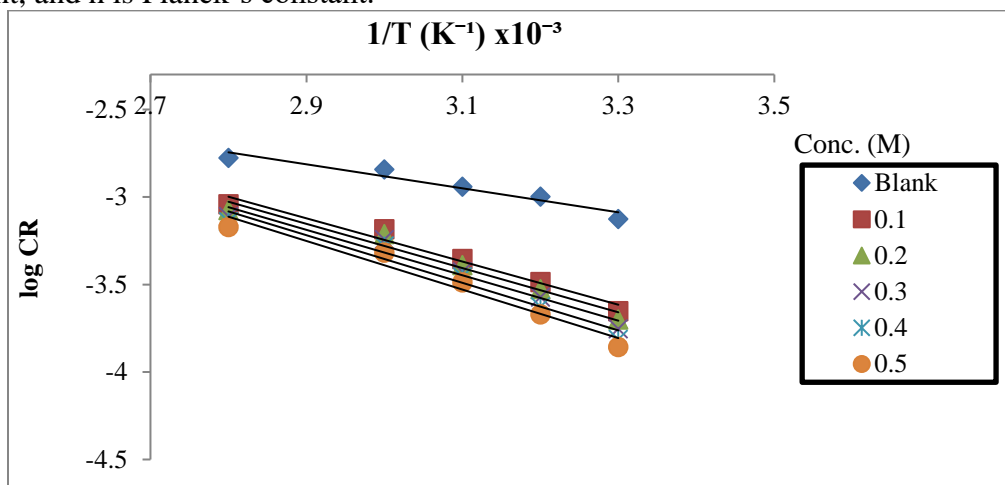


Fig. 4. Arrhenius plot of log CR vs 1/T at different extract concentrations for the corrosion of copper coupons in 2 M H₂SO₄ solution

The plot of log (CR/T) versus 1/T for the corrosion of copper in 2M H₂SO₄ containing different concentrations of AML extract was linear (Fig. 5) with a slope of $(-\Delta H^*/2.303R)$ and an intercept of $[\log (R/Nh) + \Delta S^*/(2.303R)]$ from which the values of ΔH^* and ΔS^* were computed and are shown in Table 3 The enthalpy of activation (ΔH^*) values in the absence and presence of AML extract are all positive. As reported by [Awe *et al.*, 2015; Habibat *et al.*, 2019], the positive sign of ΔH^* is related to the endothermic nature of the metal dissolution process which is attributed to physical adsorption. The positive sign of the

enthalpy of activation as obtained in the present study shows the endothermic nature of the copper dissolution process. It is also seen that ΔH^* and E_a vary in the same manner, supporting the proposed inhibition mechanism. Large and negative values of the ΔS^* in the absence and presence of the extract indicate that the activated complex in the rate-determining step represents an association rather than a dissociation step, meaning that a decrease in disorderliness takes place from reactants to the activated complex. Similar observations have been reported (Okafor *et al.*, 2012).

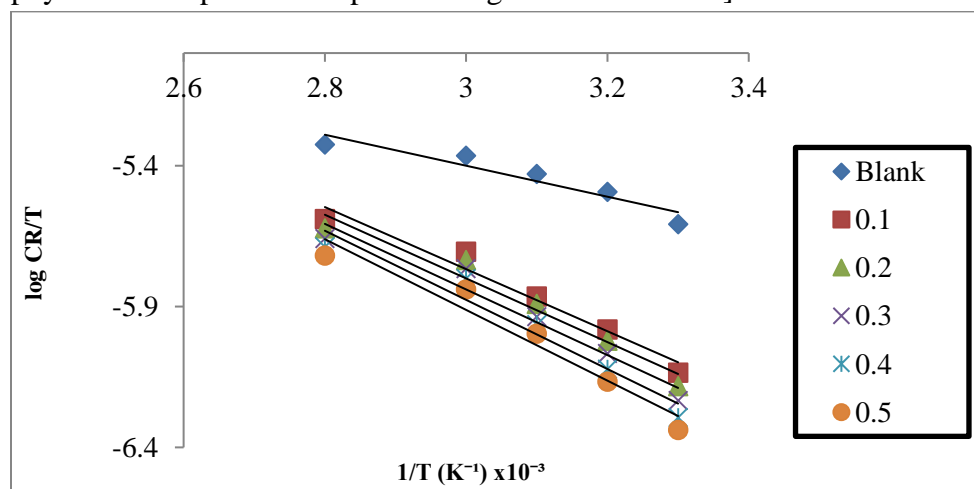


Fig.. 5. Transition plots of (log (CR/T) vs 1/T) for the corrosion of copper in 2M H₂SO₄



at different concentrations of the extract

Table 3. Thermodynamic parameter of copper in the presence of AMLE in acid medium

Conc.(g/l)	E_a (kJ/mol)	ΔH (kJ/mol)	$-\Delta S$ (kJ/mol)
Blank	12.12	10.53	134.33
0.1	22.63	21.10	110.67
0.2	23.20	21.64	109.63
0.3	23.83	22.31	108.42
0.4	25.04	23.49	105.53
0.5	27.56	24.03	104.59

3.4. Potentiodynamic Polarization (PDP) study

Potentiodynamic polarization curves for copper in 2M H₂SO₄ solution in the absence and presence of *Acanthus montanus* extract at 303K are shown in Fig. 6. The polarization parameters such as corrosion potential (E_{corr}), corrosion current density (I_{corr}), anodic Tafel slope (β_a), cathodic Tafel slope (β_c) were obtained by extrapolation of the linear Tafel sections of the anodic and cathodic curves and their values are presented in Table 4.

The potentiodynamic polarization curves and associated data provide insights into the corrosion inhibition performance of AMLE on copper in 2M H₂SO₄ medium. From the polarization parameters, it is evident that the

introduction of AMLE significantly reduces the corrosion current density (I_{corr}) compared to the blank system, indicating effective inhibition of the corrosion process. The I_{corr} for the blank is $-505 \mu\text{Acm}^2$, while at the highest concentration of AMLE (0.5 g/L), it decreases to $-494 \mu\text{Acm}^2$, corresponding to a substantial increase in inhibition efficiency (η) to 72.5%.

This reduction in I_{corr} demonstrates the protective action of AMLE, likely due to its adsorption onto the copper surface, thereby forming a barrier that minimizes direct acid-metal interaction. The cathodic Tafel slope (β_c) decreases significantly with increasing AMLE concentration, from 102 mVdec^{-1} for the blank to 28 mVdec^{-1} at 0.5 g/L.

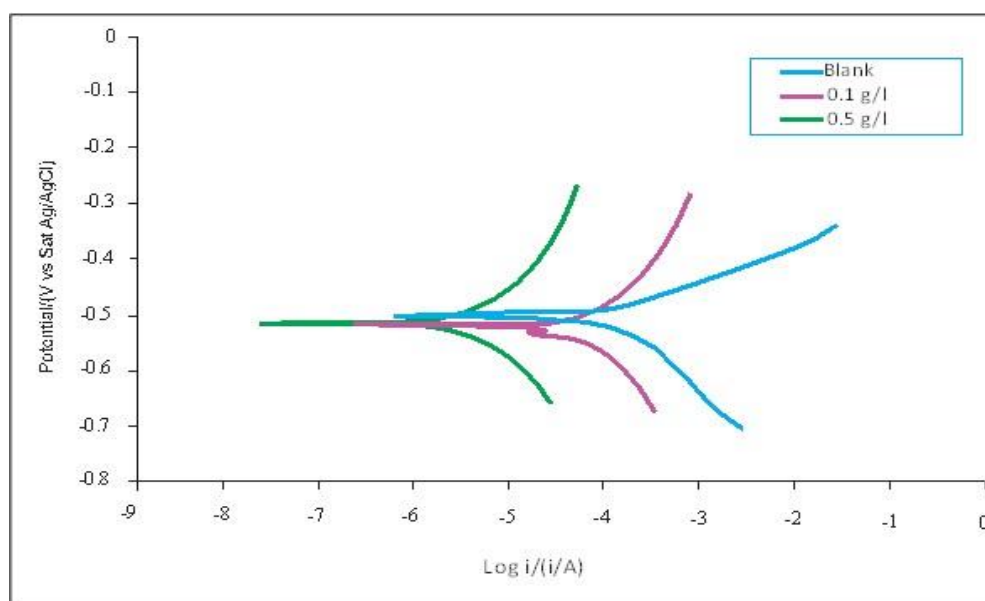


Fig. 6. Potentiodynamic Polarization Curve of the Copper in 2M H₂SO₄ in the absence and different concentrations of AMLE.

This suggests that AMLE predominantly affects the cathodic reaction, likely by hindering the hydrogen evolution process. The anodic Tafel slope (β_a) shows less variation, indicating that the anodic metal dissolution reaction is also influenced but to a lesser extent. These observations confirm that AMLE acts as a mixed-type inhibitor, with a more pronounced impact on the cathodic reaction. The corrosion potential (E_{corr}) shifts moderately in the presence of AMLE compared

to the blank system. The magnitude of these shifts is less than ± 85 mV, implying that the inhibition mechanism is dominated by physical adsorption, where weak interactions such as van der Waals forces and hydrogen bonding play a major role. However, the partial modification of both anodic and cathodic reactions, as evidenced by the changes in β_c and β_a , suggests that some degree of chemical interaction between AMLE molecules and the copper surface may also occur.

Table 4: Polarization parameters obtained at various concentrations of AMLE on copper in 2M H₂SO₄ medium.

Conc. (g/l)	E_{corr} (mV)	I_{corr} (μAcm^{-2})	β_c (mVdec ⁻¹)	β_a (mVdec ⁻¹)	η (%)
BLANK	-505	102	540	455	-
0.1	-499	50	570	440	51.0
0.5	-494	28	521	413	72.5

The significance of the differences in E_{corr} between the inhibited and blank systems further reinforces this interpretation. The moderate shifts in E_{corr} indicate that AMLE does not drastically alter the electrochemical balance between the anodic and cathodic reactions but instead provides a protective layer on the surface. This layer reduces both the anodic dissolution of copper and the cathodic hydrogen evolution, contributing to the overall inhibition efficiency.

The increasing inhibition efficiency (η) with higher AMLE concentrations highlights the concentration-dependent nature of the inhibition process. At 0.1 g/L, η is 51.0%, while at 0.5 g/L, it reaches 72.5%. This trend indicates that more inhibitor molecules adsorb onto the copper surface as the concentration increases, enhancing the protective barrier and further reducing corrosion. The analysis of the polarization parameters and the observed shifts in E_{corr} reveal that AMLE functions as a

mixed-type inhibitor with dominant physical adsorption characteristics. The reduction in I_{corr} , changes in Tafel slopes, and moderate shifts in E_{corr} collectively demonstrate that AMLE effectively mitigates copper corrosion in 2M H₂SO₄ by forming an adsorbed protective layer on the metal surface. This dual mode of action, involving both physical and partial chemical adsorption, underscores the potential of AMLE as a sustainable and efficient corrosion inhibitor in acidic environments.

3.5 Electrochemical impedance spectroscopy (EIS) measurements

The Nyquist plots for the corrosion of copper in 2M H₂SO₄ in the absence and presence of various concentrations of AMLE, as depicted in Fig. 7, exhibit semicircular profiles characteristic of a charge transfer-controlled corrosion process. This indicates that the predominant mechanism of corrosion is governed by the transfer of charge at the



metal/solution interface. The diameter of the semicircles increases in the presence of AMLE, with a further increase observed as the extract concentration rises from 0.1 to 0.5 g/L. This behavior demonstrates that AMLE forms a protective inhibitive layer on the copper surface, which becomes more robust with higher concentrations of the extract.

The charge transfer resistance (R_{ct}) values, derived from the impedance differences at lower and higher frequencies, show a significant increase with AMLE concentration. For example, the R_{ct} value increases from $108.59 \Omega \cdot \text{cm}^2$ for the blank solution to $241.89 \Omega \cdot \text{cm}^2$ and $402.61 \Omega \cdot \text{cm}^2$ for AMLE concentrations of 0.1 g/L and 0.5 g/L, respectively. This increase in R_{ct} reflects the reduced rate of the charge transfer process, confirming the formation of a protective barrier on the copper surface. The double-layer capacitance (C_{dl}), calculated using standard equations, shows an inverse trend, decreasing with higher AMLE concentrations. The reduction in C_{dl} from $3.635 \mu\text{F}/\text{cm}^2$ for the blank solution to $0.779 \mu\text{F}/\text{cm}^2$ and $0.332 \mu\text{F}/\text{cm}^2$ for 0.1 g/L and 0.5 g/L AMLE, respectively, suggests that water molecules at the metal/solution interface are gradually replaced by AMLE molecules, leading to a decrease in the dielectric constant and an

increase in the electrical double-layer thickness. These findings indicate that AMLE molecules adsorb onto the copper surface, forming a protective film that impedes mass and charge transfer processes. The adsorption process is likely facilitated by phytochemical constituents of the extract, which interact with the copper surface through chemical or physical adsorption mechanisms. This is supported by literature [Patel and Vashi, 2015; Zheng et al., 2018], which suggests that natural extracts can act as efficient inhibitors by adsorbing onto metal surfaces and forming a protective barrier. Furthermore, the inhibition efficiency ($\eta\%$) of AMLE increases with extract concentration, reaching a maximum of 73.03% at 0.5 g/L. This enhanced efficiency is attributed to increased surface coverage by the extract molecules, which block active corrosion sites on the copper surface. The correlation between extract concentration and inhibition efficiency aligns with previous studies (Muthukrishnam et al., 2014), reinforcing the potential of AMLE as an effective green inhibitor for copper corrosion in acidic environments. The results underscore the practical applicability of AMLE for environmentally friendly alternative to synthetic inhibitors.

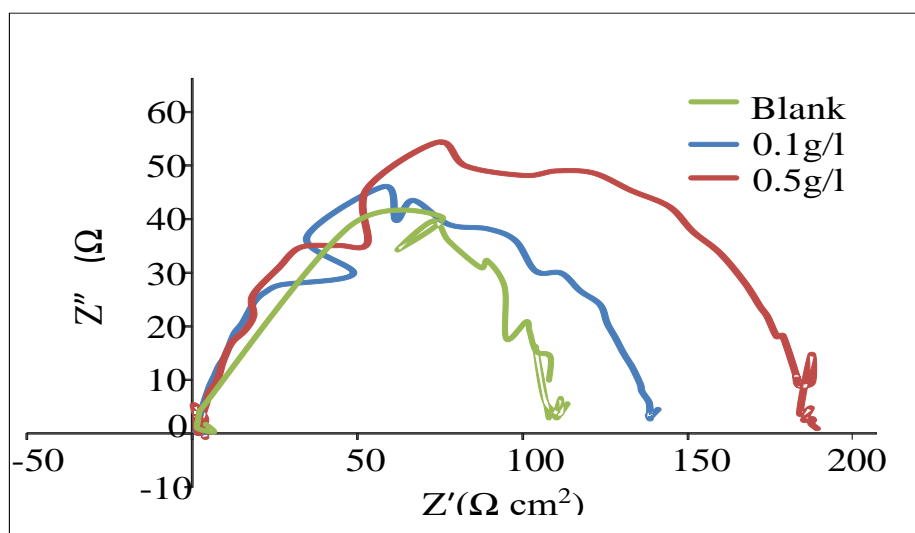


Fig.7. Nyquist plots of copper in 2M H₂SO₄ without and with various concentration of AMLE

3.6 Surface analysis

3.6.1 FT-IR Analysis

The FT-IR spectra of *Acanthus montanus* leaves extract (AMLE) and the corrosion product formed on copper in the presence of AMLE in 2M H₂SO₄ (Fig. 8) provide critical insights into the interaction between the extract's functional groups and the copper surface. Table 6 compares the wavenumbers and assigned functional groups of the pure AMLE and the corrosion product, along with

standard reference wavenumbers for these functional groups. In the pure AMLE spectrum, a broad O-H stretch at 3347.67 cm⁻¹ was observed, indicative of alcohol or hydroxyl groups. This peak shifted to 3471.98 cm⁻¹ in the corrosion product, indicating an interaction of hydroxyl groups with the copper surface. This shift suggests that the hydroxyl groups in the extract are involved in the adsorption process, contributing to the inhibition of corrosion by forming a protective layer on the copper surface.

Table 5: Impedance parameters obtained at various concentrations of AMLE on copper in 2M H₂SO₄ medium.

Extracts Conc. (g/l)	R _p (R _{ct}) Ω cm ²	f _{max} (Hz)	C _{dl} (μF/cm ²)	% IE
Blank	108.59	40.34	3.635	-
0.1	241.89	84.45	0.779	55.11
0.5	402.61	118.95	0.332	73.03

Additionally, the C-H stretch at 2926.97 cm⁻¹ in the pure extract shifted to 2951.29 cm⁻¹, and another C-H stretch at 2648.35 cm⁻¹ shifted to 2679.21 cm⁻¹ in the corrosion product. These changes align with alkanes' standard reference wavenumbers, reinforcing the idea that the alkane groups in AMLE are also participating in the adsorption mechanism. The C=O carbonyl stretch initially observed at 1600.97 cm⁻¹ in the pure extract shifted to 1726.35 cm⁻¹ in the corrosion product, indicating strong interaction between the carbonyl functional groups and the copper surface. This interaction likely leads to the formation of complexes that enhance corrosion inhibition. Interestingly, peaks corresponding to C≡C stretches (2047.51–2288.62 cm⁻¹) and C=O stretches (1826.65–1909.59 cm⁻¹) disappeared entirely in the corrosion product. This disappearance suggests the involvement of these functional groups in chemical bonding or transformation during the adsorption process.

Other shifts included the C-O stretch moving from 1149.61 cm⁻¹ to 1162.15 cm⁻¹ and the C-H bend at 883.43 cm⁻¹ shifting to 864.14 cm⁻¹. These variations in peak positions reflect structural changes caused by the interaction of AMLE components with the copper surface. New peaks, such as a C-H bend at 988.55 cm⁻¹, appeared in the corrosion product spectrum, indicating the possible formation of new molecular structures on the copper surface. Peaks such as O-H stretches (3128.64–3261.74 cm⁻¹), C≡C stretches, and certain C-N stretches disappeared in the corrosion product. This disappearance implies the involvement of these functional groups in the adsorption and bonding process, further confirming the extract's role in forming a protective layer on the copper surface (Alaneme et al., 2016; Ameh et al. ; 2017, Mahgoub et al., 2019)

The observed shifts, the appearance of new peaks, and the disappearance of others strongly suggest chemical adsorption of the AMLE on



the copper surface. The interaction involves the formation of coordinate bonds between the functional groups of AMLE and the copper atoms. These results highlight the effectiveness of AMLE as a green corrosion inhibitor, wherein its functional groups interact

chemically with the copper surface to form a stable, protective film that reduces the metal's corrosion rate. Such findings emphasize the potential of plant extracts as sustainable and eco-friendly alternatives to synthetic corrosion inhibitors.

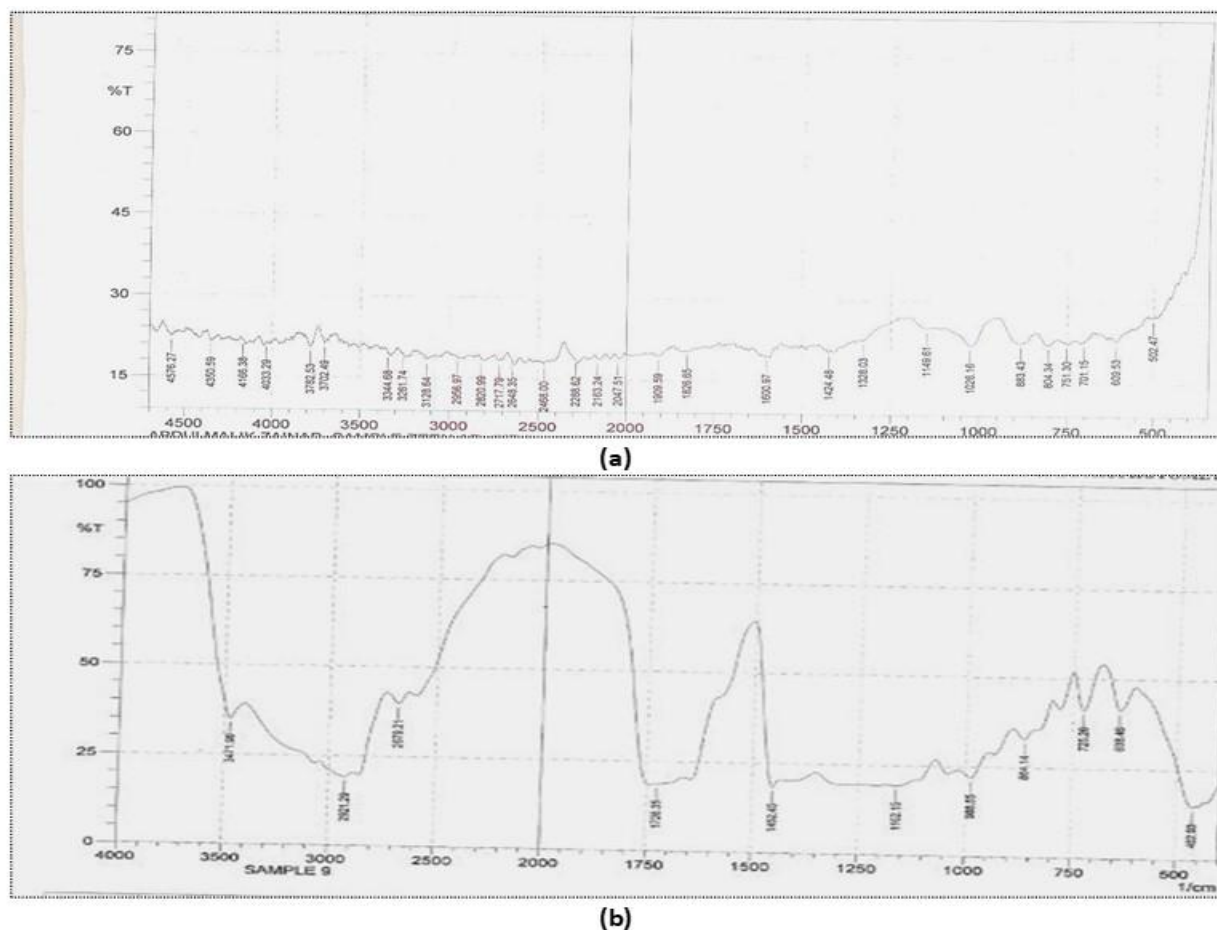


Fig.s 8: (a) FTIR spectrum of pure AMLE (b) FTIR spectrum of corrosion products on copper in H_2SO_4 solution containing 0.5g/l AMLE

3.6.2 SEM Analysis

Fig. 9 illustrates the surface morphology of copper specimens under different conditions, providing insights into the effect of AMLE (Aqueous Methanolic leaf extract) as a corrosion inhibitor in 2M H_2SO_4 . The micrograph in Fig. 9a represents the plain and polished copper surface prior to immersion. The surface is smooth and free from significant defects, pits, or roughness, reflecting the pristine condition of the metal before exposure

to the corrosive medium. This serves as the baseline for comparing the subsequent corrosion and inhibition effects. In Fig. 9b, the copper surface is shown after 18 hours of immersion in 2M H_2SO_4 in the absence of AMLE. The surface appears rough, uneven, and significantly damaged, with visible corrosion products and pits. The severity of the corrosion can be attributed to the aggressive attack by H^+ ions in the acidic medium, leading to the dissolution of copper and the formation of copper ions. The lack of a protective barrier



allows direct interaction between the copper and the acid, resulting in extensive degradation. Fig. 9c depicts the copper surface after 18 hours of immersion in 2M H₂SO₄ in the presence of 0.5 g/L AMLE. The surface is relatively smooth and exhibits less damage compared to the corroded surface in Fig. 9b. The reduction in surface roughness and the presence of a protective layer are evident. This suggests that the AMLE molecules adsorbed onto the copper surface, forming a compact and adherent inhibitive film that minimized direct contact between the metal and the acidic environment. This protective film acts as a barrier to both charge and mass transfer processes, effectively reducing the rate of corrosion. The protective effect of AMLE can be attributed to the

presence of phytochemical constituents such as alkaloids, flavonoids, and tannins, which are known to adsorb onto metal surfaces through interactions with vacant d-orbitals of the metal. The adsorption of these organic molecules likely occurs via a combination of physical and chemical adsorption mechanisms, forming a barrier that inhibits further attack by the acidic medium. This aligns with earlier findings from studies by Fouda et al. (2016), Prathiar et al., and Cookey et al. (2023), which reported the effectiveness of plant extracts in reducing corrosion rates. These studies also emphasize that plant extracts act by forming adsorbed protective films on metal surfaces, thereby minimizing corrosion in aggressive environments.

Table 6: Frequencies and intensities of IR absorption and the corrosion product on Copper i the presence of ACME as inhibitor in H₂SO₄ medium

Pure AML Extract		Corrosion Product on Copper Surface		Standard Reference Wavenumber (cm ⁻¹)
Frequency (cm ⁻¹)	Assigned Functional Groups	Frequency (cm ⁻¹)	Assigned Functional Groups	
3347.67	O-H stretch (alcohol)	3471.98	O-H stretch (alcohol)	3200–3600
3128.64 – 3261.74	O-H stretch (alcohol)	Peaks disappeared	–	3200–3600
2926.97	C-H stretch	2951.29	C-H stretch	2850–2960
2648.35	C-H stretch	2679.21	C-H stretch (alkanes)	2650–2700
2047.51 – 2288.62	C≡C stretch	Peaks disappeared	–	2100–2260
1826.65 – 1909.59	C=O stretch	Peaks disappeared	–	1700–1870
1600.97	C=O carbonyl stretch	1726.35	C=O carbonyl stretch	1650–1750
1424.48	C-H stretch (alkanes)	1452.45	C-H stretch (alkanes)	1350–1470
1149.61	C-O stretch	1162.15	C-O stretch	1050–1250
1026.16	C-N stretch	Peak disappeared	–	1020–1230
–	–	988.55	C-H bend	970–1000
883.43	C-H bend	864.14	C-H bend	850–900



701.15	C-H aliphatic	725.26	C-H aliphatic	675–725
609.47	C-H stretch	638.46	C-H stretch	600–650

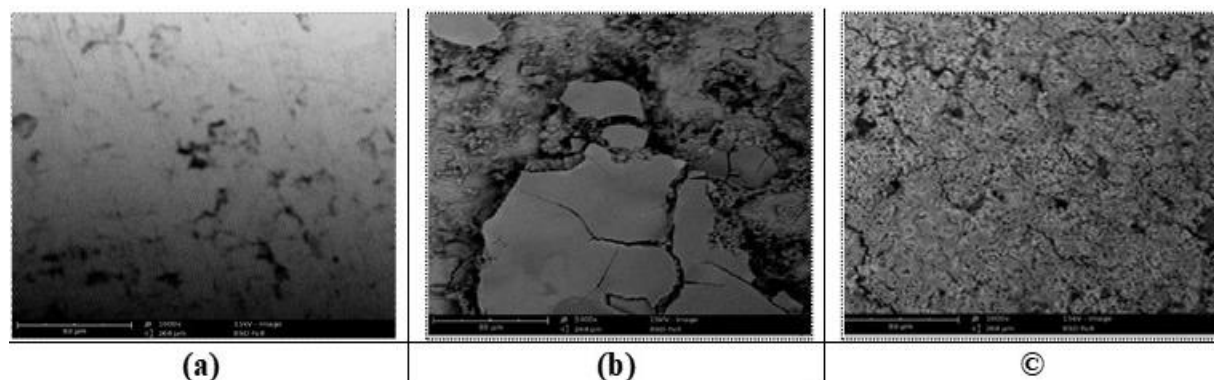


Fig. 9: SEM micrographs of (a) metal (b) metal without inhibitor (c) metal with inhibitor

The comparison between Figs. 9b and 9c clearly illustrates the effectiveness of AMLE in mitigating copper corrosion. While the surface in Fig. 9b shows severe degradation due to acid attack, the smoother morphology in Fig. 9c highlights the inhibitory action of AMLE, reducing the extent of damage and preserving the structural integrity of the copper surface. The SEM analysis conclusively demonstrates the inhibitory role of AMLE in 2M H₂SO₄. The protective film formed by the extract molecules not only reduces the extent of corrosion but also suggests its potential as an eco-friendly and cost-effective corrosion inhibitor for copper in acidic environments. These observations are further supported by the electrochemical data, which showed an increase in charge transfer resistance (R_{ct}) and a decrease in double-layer capacitance (C_{dl}) with increasing concentrations of the extract, confirming the protective nature of AMLE. These results are consistent with studies by Patel and Vashi (2015), Zheng et al. (2018), and Muthukrishnam et al. (2014), reinforcing the practical application of AMLE as a green corrosion inhibitor.

4.0 Conclusion

The study investigated the corrosion inhibition effect of *Acanthus montanus* leaf extract (AMLE) on copper in 2M H₂SO₄ using weight

loss, potentiodynamic polarization (PDP), electrochemical impedance spectroscopy (EIS), and thermodynamic analysis. The results

demonstrated that AMLE significantly reduces the corrosion rate of copper, with inhibition efficiency increasing with higher extract concentrations. Weight loss measurements indicated a maximum inhibition efficiency of 72.5% at 0.5 g/L of AMLE, consistent with data obtained from PDP and EIS analyses. Thermodynamic investigations revealed that the apparent activation energy (E_a) increased in the presence of AMLE, indicating a physical adsorption mechanism. The values of enthalpy (ΔH*) were positive, confirming the endothermic nature of the copper dissolution process, while negative entropy (ΔS*) values suggested an ordered association at the metal-solution interface during the formation of the activated complex. PDP studies confirmed that AMLE acts as a mixed-type inhibitor, with a greater effect on the cathodic reaction, as evidenced by the significant decrease in the cathodic Tafel slope (β_c). The adsorption of AMLE molecules onto the copper surface provided a protective layer that hindered mass and charge transfer, thereby reducing both anodic and cathodic reactions.

EIS measurements supported the charge transfer-controlled corrosion mechanism, with



larger semicircle diameters observed in the presence of AMLE, reflecting increased charge transfer resistance (R_{ct}). The enhanced R_{ct} values at higher AMLE concentrations indicated the formation of a more robust barrier on the copper surface. The adsorption process was further validated by fitting data to the Langmuir isotherm, confirming that AMLE molecules physically adsorb onto the copper surface through weak interactions such as van der Waals forces and hydrogen bonding. In conclusion, the study demonstrated that AMLE effectively inhibits the corrosion of copper in acidic environments through the formation of an adsorbed protective layer. The thermodynamic and electrochemical analyses confirmed the physical adsorption mechanism, supported by increased E_a and positive ΔH^* values. AMLE's dual action on anodic and cathodic reactions underscores its potential as a sustainable and eco-friendly corrosion inhibitor for industrial applications.

It is recommended that further studies explore the isolation and characterization of active phytochemical components in AMLE responsible for corrosion inhibition. Additionally, testing the inhibitor's performance in other corrosive environments and at varying temperatures would provide a broader understanding of its applicability. Industrial-scale testing of AMLE as a corrosion inhibitor in pipelines and storage tanks is also encouraged to validate its practical use and scalability.

5.0 References

- Abeng, F. E., Idim, V. D., & Nna, P. J. (2017). Kinetics and thermodynamic studies of corrosion inhibition of mild steel using methanolic extract of *Erigeron floribundus* (Kunth) in 2 M HCl solution. *World News of Natural Sciences*, 10, pp. 26–38.
- Abiola, O. K., Abdulraman, O. C. A. & Suleiman, M. (2016). Eco-friendly corrosion inhibitors: Effect of delonixregia extract on corrosion and kinetics of corrosion process of aluminum alloy 2S in HCl solution. *African Corrosion Journal*, 2, 2, pp. 11-16.
- Alaneme, K. K., Olusegun S .J. & Adelowo O.T. (2016). Corrosion inhibition and adsorption mechanism studies of Hunteria umbellate seed husk extracts on mild steel in acidic solutions. *Alexandria Eng J.* 55, 1, pp. 673-681.
- Ameh, O. P., Kolo, A. M., Ahmed, A., & Ajanaku, I. K. (2017). Electrochemical study of the corrosion inhibition of *Delonix regia* for mild steel in sulphuric acid medium. *Journal of Industrial and Environmental Chemistry*, 1, 1, pp. 15–21.
- Eddy, N. O., Ameh, P. O. and Essien, N. B. (2018). Experimental and computational Chemistry studies on the inhibition of aluminum and mild steel in 0.1 M HCl by 3-nitrobenzoic acid. *Journal of Taibah University for Science*, 12, 5, pp. 545-556. , <https://doi.org/10.1080/16583655.2018.1500514>
- Anadebe, V. C., Onukwuli, O. D., Omotioma, M., & Okafor, N. A. (2018). Optimization and electrochemical study on the control of mild steel corrosion in hydrochloric acid solution with bitter kola leaf extract as inhibitor. *South African Journal of Chemistry*, 71, pp. 51–61.
- Awe, I. C., Abdulrahman, A. S., Ibrahim, H. K., Kareem, A. G., & Adams, S. M. (2015). Inhibitive performance of bitter leaf root extract on mild steel corrosion in sulphuric acid solution. *American Journal of Materials Engineering and Technology*, 3, 2, pp. 35–45.
- Bilgiç, S. (2023). Plant extracts as corrosion inhibitors against copper corrosion – An overview. *International Journal of Corrosion and Scale Inhibition*, 12, 3, pp. 1224–1260.
- Cookey, G. A., Udom, I. G., BoEkom, E. J., & Ameh, P. O. (2023). Adsorption and corrosion inhibition behavior of *Acanthus montanus* leaves extract on mild steel in sulphuric acid medium. *Catalysis Research*, 3, 3, pp. 16.



- Deepa, R. P., & Selvaraj, S. (2010). Emblica Officinalis (AMLA) leaves extract as corrosion inhibitor for copper and its alloy (Cu-27Zn) in natural sea water. *Archives of Applied Science Research*, 2, 6, pp. 140-150.
- Ebenso, E. E., Alemu, H., Umoren, S. A. & Obot, I.B. (2008) . Inhibition of mild steel corrosion in sulphuric acid using alizarin yellow gg dye and synergistic iodide additives. *International Journal of Electrochemical Science*. 3, pp. 1325 – 1339.
- Ebenso, E. E., Alemu, H., Umoren, S. A., & Obot, I. B. (2008). Inhibition of mild steel corrosion in sulphuric acid using alizarin yellow GG dye and synergistic iodide additives. *International Journal of Electrochemical Science*, 3, pp. 1325-1339.
- Ech-chihbi, E., Salim, R., Ouakki, M., Koudad, M., Guo, L., Azam, M., Benchat, N., Rais, Z., & Taleb, M. (2023). Corrosion resistance assessment of copper, mild steel, and aluminum alloy 2024-T3 in acidic solution by a novel imidazothiazole derivative. *Materials Today Sustainability*, 24, 100524. <https://doi.org/10.1016/j.mtsust.2023.100524>.
- Eddy, N. O., & Ebenso, E. E. (2010). Quantum chemical studies on the inhibition potentials of some penicillin compounds for the corrosion of mild steel in 0.1 M HCl. *Journal of Molecular Modeling*, 16, pp. 1291-1306. DOI:10.1007/S00894-0090635-6.
- Eddy, N. O. and Ebenso, E. E. (2008). Adsorption and inhibitive properties of ethanol extract of *Musa sapientum* peels as a green corrosion inhibitor for mild steel in H₂SO₄. *African Journal of Pure and Applied Chemistry* 2, 6, pp. 1-9.
- Eddy, N. O., Ibok, U. J., Garg, R., Garg, R., Falak, A. I., Amin, M., Mustafa, F., Egilmez, M., & Galal, A. M. (2022). A brief review on fruit and vegetable extracts as corrosion inhibitors in acidic environments of steel in acidic environment. *Molecules*, 27, 2991. <https://doi.org/10.3390/molecules27092991>.
- Eddy, N. O. and Ita, B. I. (2011). Experimental and theoretical studies on the inhibition potentials of some derivatives of cyclopenta-1,3-diene. *International Journal of Quantum Chemistry* 111, 14, pp. 3456-3473. DOI:10.1002/qua
- Eddy, N. O., Odoemelam, S. A., Ogoko, E. C. & Ita, B. I. (2010). Inhibition of the corrosion of zinc in 0.01 to 0.04 M H₂SO₄ by erythromycin. *Portugaliae Electrochimica Acta*, 28, 1, pp. 15-26.
- Emrayed, H. F., Amraga, E. A., Ibrahim, D. M., & Fouda, A. E. S. (2025). Corrosion inhibition effect of Schiff base and its metal complexes with [Mn (II) and Cu (II)] on carbon steel in hydrochloric acid solution: Experimental and surface studies. *International Journal of Electrochemical Science*, 20, 1, pp. 100912. <https://doi.org/10.1016/j.ijoes.2024.100912>.
- Fadare, O. O., Okoronkwo, A. E. & Olasehinde E. F. (2016). Assessment of anticorrosion potentials of extract of *Ficus asperifolia-Miq* (Moraceae) on mild steel in acidic medium. *African Journal of Pure and Applied Chemistr.*, 10, 1, pp. 8- 22.
- Fadel W., Mahmoud A.A. & Ghassab M.A. (2017). Corrosion inhibition of copper by *Capparis spinosa* L extract in strong acidic medium: Experimental and Density Functional Theory. *Int. J. of Elect. Sci.*, 12, pp.4664-4676.
- Folorunso, O. (2023). *Mitigation of microbially induced concrete corrosion: Quantifying the efficacy of surfac treatments using ASTM standards* (Doctoral dissertation). Youngstown State University.
- Fouda A. S., Mohamed A. E. & Khalid M. A. (2016). *Trigonella stellate* extract as corrosion inhibitor for Copper in 1M nitric acid solution. *Journal of Chem. and Pharm. Research*. 8, 2, pp. 86-98.
- Fouda, A. S., Elmorsi, M. A. & Abou-Elmagol, B. S. (2017). Adsorption and



- inhibitive properties of Methanol extract of *Euphorbia heterophylla* for the corrosion of copper in 0.5M nitric acid solutions. *Polish Journal of Pure and Applied Sciences.*, 19, 1, pp. 95-103.
- Gapsari, F., Hadisaputra, S., Sulaiman, A. M., Ebenso, E., Thakur, A., & Kumar, A. (2024). Eco-friendly corrosion inhibition of copper in NaCl media using *Persea americana* extract: Insights from quantum and electrochemical studies. *Results in Surfaces and Interfaces*, 17, 100327. <https://doi.org/10.1016/j.rsurfi.2024.100327>.
- Habibat, F. C., David, T. O., & Taiwo, A. G. (2019). Influence of *Cissus populnea* stem extract on kinetics and thermodynamics of mild steel corrosion in acidic medium. *Ovidius University Annals of Chemistry*, 30, 1, pp. 14–20.
- Hart K.G., Orubite-Okorosaye K. & James A.O. (2016). Corrosion inhibition of copper in sea water by *Xanthosoma Spp* leaf extracts (XLE). *Int. J. of Adv. Research in Chem. Sci. (IJARCS)*. 3(12), 34-40.
- Hart, K., & James, A. O. (2014). The inhibitive effect of *Aloe vera* Barbadosensis gel on copper in hydrochloric acid medium. *Journal of Engineering and Applied Science*, 5, 1, pp. 24-49.
- Ijuo G.A., Chahul H.F. & Eneji I.S. (2016). Kinetic and Thermodynamic Studies of Corrosion Inhibition of Mild Steel using *Bridelia ferruginea* Extract in Acidic Environment. *Journal of Advanced Electrochemistry* 2, 3, pp. 107–112.
- Jonathan, M. N., Efiok, J. A. & Adeyemi, O.O. (2015). Inhibition and Adsorption-kinetic studies of *Gmelina arborea* fruit extracts on corrosion of armour steel plate in hydrochloric acid. *International Journal of Science and Engineering Research.*, 6, 9, pp. 701-717.
- Leelavathi, S., & Rajalakshmi, R. (2013). *Dodonaea viscosa* leaves extract as acid corrosion inhibitor for mild steel: A green approach. *Journal of Materials and Environmental Science*, 14, 5, pp. 625–638.
- Mahgoub, F. M., Hefnawy, A. M., & Abd Alrazzaq, E. H. (2019). Corrosion inhibition of mild steel in acidic solution by leaves and stems extract of *Acacia nilotica*. *Desalination and Water Treatment*, 169, pp. 49–58. <https://doi.org/10.5004/dwt.2019.24681>
- Mohsin, E. A., Husam, M. K. & Rasha, N.A. (2014). Inhibition of copper corrosion in H₂SO₄, NaCl and NaOH solutions by *Citrullus colocynthis* fruits extracts. *Journal of Natural Science Research*, 4, 17, pp. , 60-73.
- Mounir F., El Issami S., Bazzi Lh., Salghi R., Bammou L., Bazzi L., Chihab E.A & Jbara O. (2012). Copper corrosion behaviour in phosphoric acid containing chloride and its inhibition by *Artemisia* oil. *Int. J. of Research and Rev. in Appl. Sci. (IJRRAS)*. 13, 2, pp. 574-587.
- Mounir, F., El Issami, S., Bazzi, Lh., Salghi, R., Bammou, L., Bazzi, L., Chihab, E. A., & Jbara, O. (2012). Copper corrosion behaviour in phosphoric acid containing chloride and its inhibition by *Artemisia* oil. *International Journal of Research and Reviews in Applied Sciences*, 13, 2, pp. 574-587.
- Muthukrishnam, P., Jeyaprabha, B. & Prakash, P. (2014). Mild steel corrosion inhibition by aqueous extract of *Hyptis suaveolens* leaves. *Inter. Journal of Ind. Chem.*, 5, 5. <https://doi.org/10.1007/s40090-014-0005-9>
- Namrata, C., Dileep, K.Y., Vinad K. S. & Qurashi, M. A. (2015). A comparative study of leaves extracts for corrosion inhibitors effect on aluminium alloy in alkaline medium. *Ain Shams Eng J.* 8, 2, pp. 1-10.
- Odoemelam, S. A., Ogoko, E. C., Ita, B. I. & Eddy, N. O. (2009). Inhibition of the corrosion of zinc in H₂SO₄ by 9-deoxy-9a-aza-9a-methyl-9a-homoerythromycin A (azithromycin). *Portugaliae Electrochimica Acta*, 27, 1, pp. 57-68.



- Odoemelam, S. A. and Eddy, N. O. (2008). Effect of pyridoxal hydrochloride-2, 4-dinitrophenyl hydrazone on the corrosion of mild steel in HCl. *Journal of Surface Science and Technology* 24, 1-2, pp 1-14.
- Okafor, P. C., Ebiekpe, V. E., Azike, C. F., Egbung, G. E., Brisibe, E. A., & Ebenso, E. E. (2012). Inhibitory action of *Artemisia annua* on the corrosion of mild steel in H₂SO₄ acid solution. *International Journal of Corrosion*, 1, 8, pp. 1-8. <https://doi.org/10.1155/2012/768729>
- Okoye, C. O., Odette, F., Bello, A., Itodo, J. E., Onche, E. O., & Eddy, N. O. (2024). Metronidazole mediated potassium iodide as high-performance deterioration retardant for mild steel in an acidic media. *Journal of Dispersion Science and Technology*. <https://doi.org/10.1080/01932691.2024.2348493>.
- Oubahou, M., El Aloua, A., Benzbiria, N., El Harrari, S., Takky, D., Naimi, Y., Zeroual, A., Wang, S., Syed, A., & Belghiti, M. E. (2024). Electrochemical, thermodynamic, and computational investigation of the use of an expired drug as a sustainable corrosion inhibitor for copper in 0.5 M H₂SO₄. *Materials Chemistry and Physics*, 323, 129642. <https://doi.org/10.1016/j.matchemphys.2024.129642>.
- Patel, K. K., & Vashi, R. T. (2015). *Azadirachta indica* extract as corrosion inhibitor for copper in nitric acid medium. *Research Journal of Chemical Sciences*, 5, 11, pp. 59-66.
- Pratihari, P. S., Monika, P. S., & Alka, S. (2015). *Capparia decidua* seeds: Potential green inhibitor to combat acid corrosion of copper. *Rasayan Journal of Chemistry*, 8, 4, pp. 411-421.
- Udom, I. G., Cooney, G. A. & Abia A. A. (2017). The Effect of *Acanthus montanus* leaves Extract on corrosion of Aluminium in Hydrochloric acid medium. *Current J. of Appl. Sci. and Tech.*, 25, 2, pp. 1-11.
- Udom, I. G., Cooney, G. A. & Abia, A. A. (2018). Corrosion inhibition and adsorption characteristics of myrianthus aboreus leaves extract on copper in sulphuric acid solution. *Chemical Science International*,. 23, 3, pp. 1-13.
- Udongwo, A., & Folorunso, O. (2025). Resource recovery from maize biomass for the synthesis of SiO₂ nanoparticles and crystallographic analysis for possible applications. *Communication in Physical Sciences*, 12, 2, pp. 276-293.
- Yadav, S., Raman, A. P. S., Singh, M. B., Massey, I., Singh, P., Verma, C., & AlFantazi, A. (2024). Green nanoparticles for advanced corrosion protection: Current perspectives and future prospects. *Applied Surface Science Advances*, 21, 100605. <https://doi.org/10.1016/j.apsadv.2024.100605>.
- Yiase, S. G., Adejo, S.O., Tyohemba, T.G., Ahile, U.J.& GbertyoJ.A. (2014). Thermodynamic, Kinetic and Adsorptive Parameters of Corrosion Inhibition of Aluminium Using *Sorghum bicolor* Leaf Extract in H₂SO₄ solution. *International Journal of Advanced Research in Chemical Science*, Vol. 1, 2.
- Zheng, X., Gong, M., Li, Q., & Guo, L. (2018). Corrosion inhibition of mild steel in sulfuric acid solution by loquat (*Eriobotrya japonica* Lindl.) leaves extract. *Scientific Reports*, 8, pp. 9140. <https://doi.org/10.1038/s41598-018-27257-9>.

Compliance with Ethical Standards

Declaration

Ethical Approval

Not Applicable

Competing interests

The authors declare that they have no known competing financial interests

Funding

All aspect of the work was carried out by the author



Authors' Contribution

All components of the work were carried out by the author. Ini Udom designed and carried out the work under the supervision of Grace Cookery while Paul Ameh was involved in the experimental reporting

